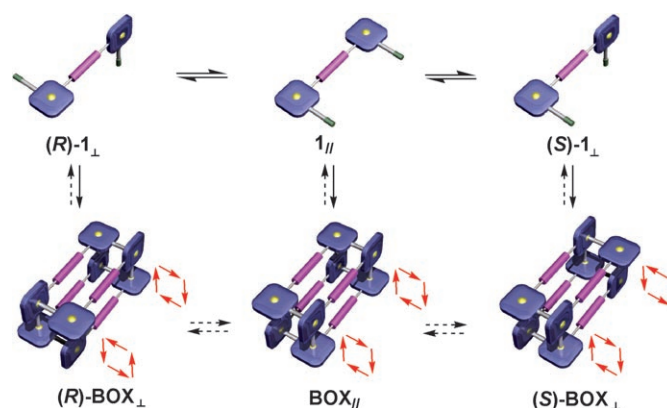
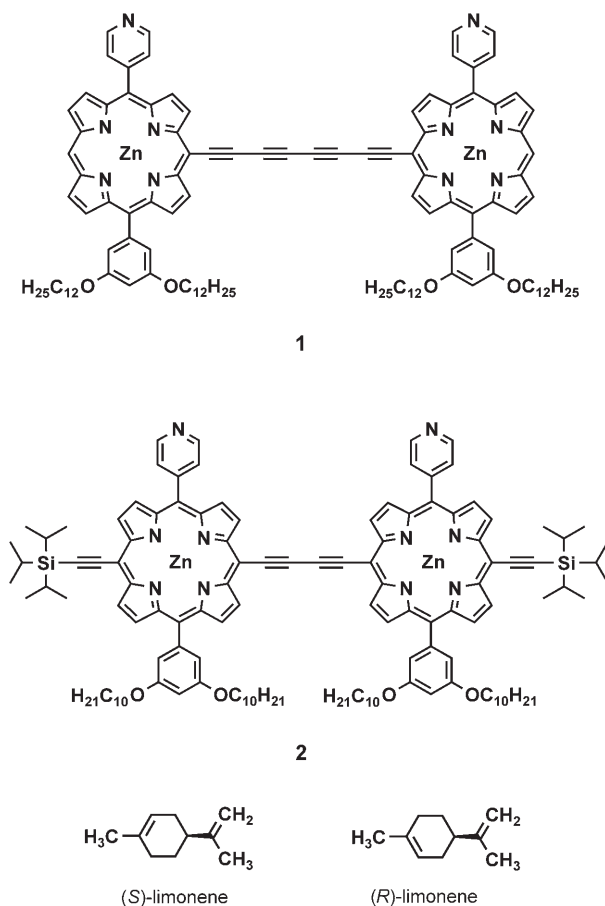


Chiroptical Sensing of Asymmetric Hydrocarbons Using a Homochiral Supramolecular Box from a Bismetalloporphyrin Rotamer

Junko Aimi, Kazumasa Oya, Akihiko Tsuda,* and Takuzo Aida*

Molecular recognition of hydrocarbons is one of the challenging subjects in supramolecular chemistry.^[1,2] Here we describe the chiroptical sensing of asymmetric hydrocarbons with an achiral organic dye molecule that self-assembles to form a box-shaped chiral cyclic tetramer.^[3,4] Chiroptical sensing of asymmetric molecules is a method in which a chromophoric host is allowed to interact with a chiral guest.^[5–11] When the chiral guest is appropriately associated with the host molecule through multipoint interactions,^[12] the host displays a circular dichroism (CD) response in the visible absorption region, which can be diagnosed without interference from other coexisting molecules. Here, the sign and intensity of the CD response reflects the absolute configuration and enantiomeric purity, respectively, of the chiral guest.^[13] For chiroptical sensing of asymmetric hydrocarbons, only limited examples have so far been reported,^[2] since these compounds do not possess appropriate functionalities for directional multipoint interactions.^[1]

Our strategy for chiroptical sensing makes use of a box-shaped chiral supramolecular assembly of the bismetalloporphyrin rotamer **1**.^[3,14,15] In the presence of an asymmetric hydrocarbon, such as limonene, enrichment of either of the two enantiomeric forms of the chiral box takes place, thereby allowing an enhanced CD response in the visible absorption region. This is based on our recent finding that the zinc complex of dialkynylene-linked bisporphyrin **2** with meso pyridyl groups self-assembles to form a box-shaped cyclic tetramer (BOX), where **2** as the building block adopts either a planar (\parallel) or a perpendicular (\perp) conformation (Scheme 1).^[3] While BOX $_{\parallel}$ consisting of the planar conformer of **2** (**2** $_{\parallel}$) is achiral, BOX $_{\perp}$ composed of its perpendicular conformer (**2** $_{\perp}$) is chiral (homochiral). Since only the latter assembly is eligible for chiroptical sensing, we synthesized **1**, a new tetraalkynylene version of **2**, with an expectation that the



Scheme 1. Schematic representations of rotamer **1** and its self-assembling event. Pink cylinders represent spacers consisting of oligoalkynylene units, while red arrows indicate the direction of Py \rightarrow Zn coordination.

[*] J. Aimi, K. Oya, Dr. A. Tsuda, Prof. Dr. T. Aida
Department of Chemistry and Biotechnology
School of Engineering
The University of Tokyo
7-3-1 Hongo, Bunkyo-ku, Tokyo 113-8656 (Japan)
Fax: (+81) 3-5841-7310
E-mail: tsuda@macro.t.u-tokyo.ac.jp
aida@macro.t.u-tokyo.ac.jp
Homepage: <http://macro.chem.t.u-tokyo.ac.jp/>
J. Aimi, Dr. A. Tsuda
PRESTO
Japan Science Technology Agency (JST)
4-1-8 Honcho, Kawaguchi, Saitama 332-0012 (Japan)

Supporting information for this article is available on the WWW under <http://www.angewandte.org> or from the author.

energetic demand for the planarization of **1**, leading to achiral BOX_{\parallel} , must be lower than that for **2**.

The tetraalkynylene-linked zinc porphyrin dimer **1** was synthesized by a procedure similar to that reported for **2**.^[3b] The ^1H NMR spectrum and the absorption and emission spectral features of **1**, along with its size-exclusion chromatographic profile (SEC),^[16] indicate that **1** self-assembles to form a box-shaped cyclic tetramer in a manner analogous to the self-assembly of **2**.^[3,17] In CDCl_3 at 20°C , compound **1** shows two Soret absorption bands at 458 and 485 nm, assignable to BOX_{\perp} and BOX_{\parallel} , respectively, where the molar ratio $\text{BOX}_{\perp}/\text{BOX}_{\parallel}$, as determined by ^1H NMR spectroscopy, is nearly unity.^[18] To our surprise, the supramolecular assemblies of **1** are rather resistant to dissociation, and the enantiomers of BOX_{\perp} were successfully separated from one another by means of chiral HPLC on a SUMICHIRAL OA-3100 column using $\text{CH}_2\text{Cl}_2/\text{hexane}$ (3:7) as the eluent.^[17b,19] When the chiral HPLC profile of self-assembled **1** was traced at 20°C by the absorbance change at 455 nm mostly due to BOX_{\perp} , two elution peaks appeared at 6.1 and 8.5 min (Figure 1a). By monitoring the CD intensity change at 455 nm, the former and latter elution peaks were found to exhibit responses of positive and negative sign, respectively. On the other hand, an HPLC trace recorded by monitoring the absorbance change at 485 nm due to BOX_{\parallel} displayed only a single elution peak (Figure 1b). Apparently the two elution peaks in Figure 1a can be assigned to the enantiomers of

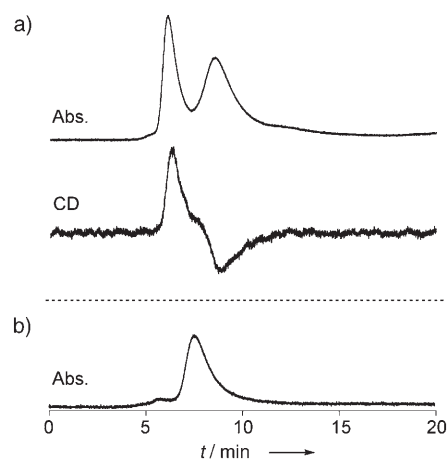


Figure 1. Chiral HPLC profiles of self-assembled **1** using $\text{CH}_2\text{Cl}_2/\text{hexane}$ (3:7) as an eluent at 20°C , monitored by absorption (and CD) responses at a) 455 and b) 485 nm.

homochiral BOX_{\perp} consisting of the perpendicular conformer of **1** ($\mathbf{1}_{\perp}$), while the single elution peak in Figure 1b is due to achiral BOX_{\parallel} composed of the planar conformer of **1** ($\mathbf{1}_{\parallel}$). In fact, the two fractions of BOX_{\perp} in Figure 1a, after chromatographic isolation, displayed mirror-image CD spectra (Figure 2c and e), whereby a very large CD spectral intensity of the first fraction is noteworthy. By reference to Figure 2b, the

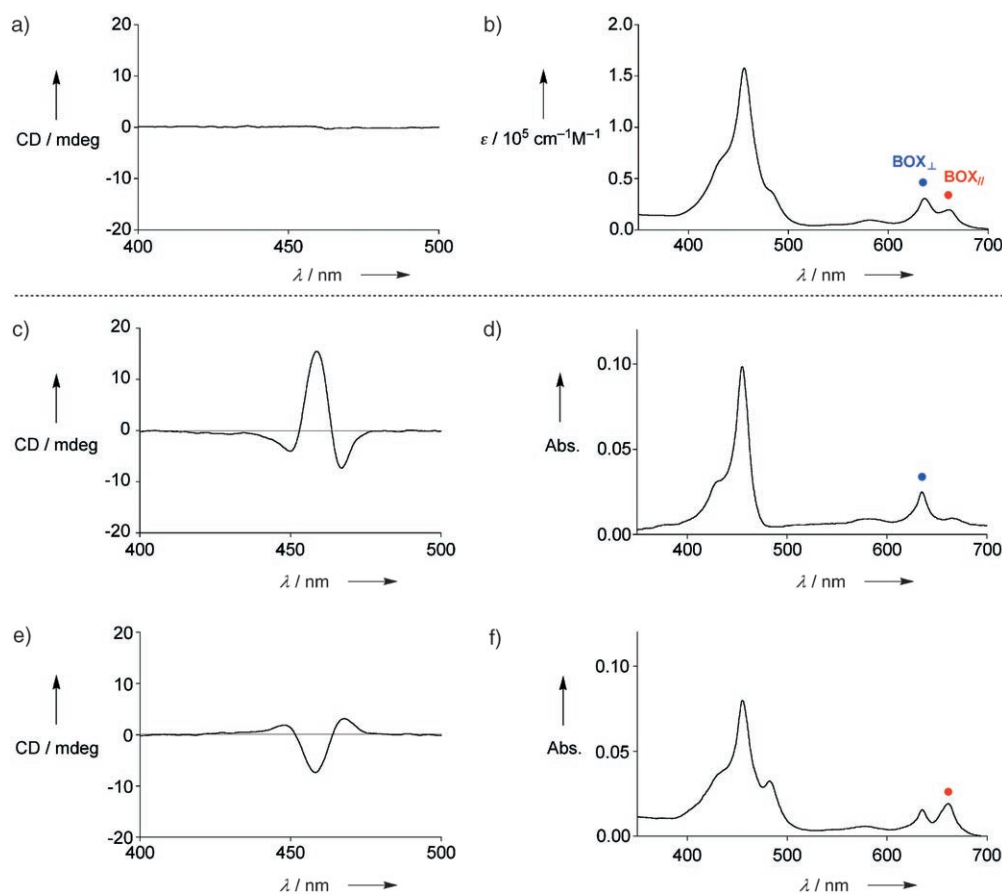


Figure 2. CD and absorption spectra of self-assembled **1** in $\text{CH}_2\text{Cl}_2/\text{hexane}$ (3:7) at 20°C before (a,b) and after chiral HPLC with $\text{CH}_2\text{Cl}_2/\text{hexane}$ (3:7) as an eluent (first (c,d) and second (e,f) fractions). Blue and red dots mark the Q-bands of BOX_{\perp} and BOX_{\parallel} , respectively.

absorption spectrum of the first fraction predominantly contains only one set of the zinc porphyrin Soret and Q-bands assignable to BOX_{\perp} (Figure 2d),^[3] while that of the second fraction appears to include, besides the above set, another set of these absorption bands, assignable to BOX_{\parallel} (Figure 2f). Considering also the fact that the CD spectral intensity of the second fraction (Figure 2e) is much lower than that of the first fraction (Figure 2c), the second fraction is apparently contaminated with achiral BOX_{\parallel} as well as the enantiomeric counterpart of homochiral BOX_{\perp} . Judging from the intense CD spectrum of the first fraction, homochiral BOX_{\perp} can be characterized by a very large molar molecular ellipticity. In fact, at the absorption maximum of the Soret band (458 nm), $|\Delta\epsilon|$ of BOX_{\perp} is estimated to be at least $3640 \text{ cm}^{-1}\text{M}^{-1}$ ($910 \text{ cm}^{-1}\text{M}^{-1}$ per unit of $\mathbf{1}_{\perp}$).^[20]

We found that the chiroptical activity of BOX_{\perp} at ambient temperatures lasts for a rather long period of time. For example, in CH_2Cl_2 /hexane (3:7) at 20°C , the CD intensity of BOX_{\perp} (first fraction in chiral HPLC) decreased only slowly with a half-life ($t_{1/2}$) of 11.5 h (Figure 3a), where the pseudo-first-order rate constant, as estimated from the initial slope of the racemization, was $1.67 \times 10^{-5} \text{ s}^{-1}$ ($r^2 = 0.999$). On the other hand, when the sample was heated to 50°C , $t_{1/2}$ was considerably shortened to 15 min. Arrhenius plots of the kinetic data obtained at 10 – 50°C provided an activation energy for the racemization of 97.5 kJ mol^{-1} (Figure 3b). Such a large thermodynamic stability of BOX_{\perp} most likely arises from the eight Zn–N coordination bonds involved. Nevertheless, addition of a coordinating base, such as pyridine, to the sample solution resulted in rapid disappearance of its

chiroptical activity as a result of the accelerated dissociation and reassembly of the building block.

The dynamic self-assembling behavior of $\mathbf{1}$ to form homochiral BOX_{\perp} , thus observed, prompted us to explore its potential for the chiroptical sensing of asymmetric hydrocarbons. For this purpose we chose limonene, since both enantiomers are available. Electronic absorption spectroscopy of a (*R*)-limonene solution of $\mathbf{1}$ (3.0 mL ; $[\mathbf{1}] = 6.24 \times 10^{-6} \text{ M}$), which was allowed to stand for 1 day at 20°C , showed a Soret absorption band at 458.5 nm characteristic of BOX_{\perp} with a red-shifted shoulder at 487.5 nm due to BOX_{\parallel} . While (*R*)-limonene is chiroptically silent in the visible absorption region, the (*R*)-limonene solution of $\mathbf{1}$ displayed clear CD bands at 440 – 480 nm (Figure 4a, solid curve) with split Cotton effects [$\lambda_{\text{max}} = 468$ ($\theta = +2.0$), 460 (-5.5), and 451 nm ($+2.3 \text{ mdeg}$)]. Use of (*S*)-limonene as the solvent resulted in a mirror-image CD spectrum (broken curve) of BOX_{\perp} observed in (*R*)-limonene. These CD spectral features are essentially identical to those of the chromatographically isolated enantiomers of BOX_{\perp} (Figure 2), indicating that either of the two enantiomers of BOX_{\perp} is thermodynamically enriched in limonene depending on its absolute configuration.

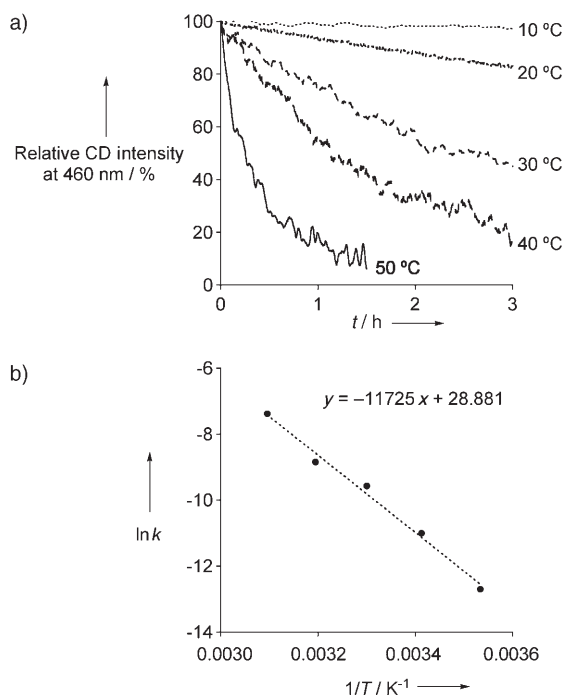


Figure 3. a) Time-dependent changes in CD intensity at 460 nm of BOX_{\perp} from $\mathbf{1}$, obtained as the first fraction in chiral HPLC, at 10 – 50°C in CH_2Cl_2 /hexane (3:7). b) Arrhenius plot of the pseudo-first-order rate constants of racemization obtained from (a).

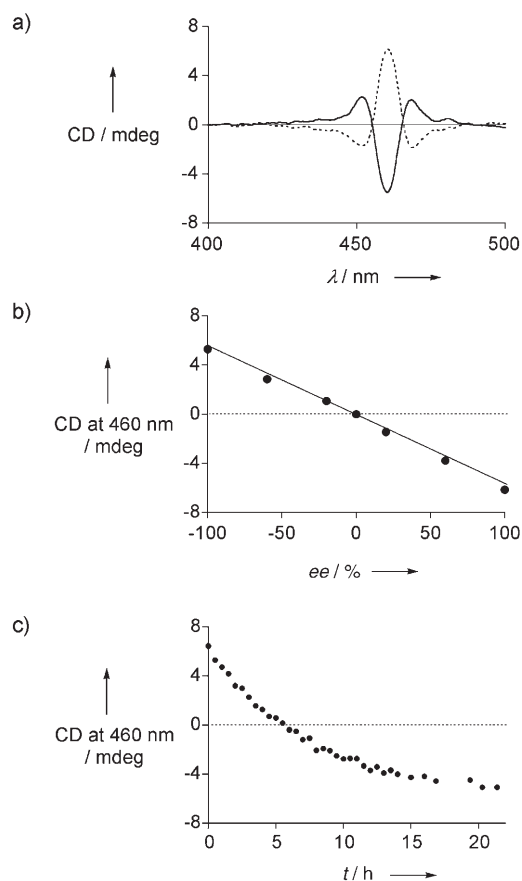


Figure 4. a) CD spectra of $\mathbf{1}$ ($6.2 \times 10^{-6} \text{ M}$) at 20°C in (*R*)- and (*S*)-limonene (solid and broken line, respectively). b) CD intensity at 460 nm of $\mathbf{1}$ as a function of the enantiomeric excess (%) of limonene. c) Plots of CD intensity at 460 nm after 100-fold dilution of a (*S*)-limonene solution of $\mathbf{1}$ (0.03 mL , $[\mathbf{1}] = 6.2 \times 10^{-4} \text{ M}$) with 3.0 mL of (*R*)-limonene.

As shown in Figure 4b, when **1** was dissolved in limonene at varying molar ratios of its enantiomers, the observed CD intensity of the resulting solution at, for example, 460 nm changed in linear proportion to the enantiomeric excess of limonene. Thus, the enantiomeric purity of limonene can be readily determined. In relation to this result, upon 100-fold dilution of a (*S*)-limonene solution of **1** (30 μ L, [**1**] = 6.2×10^{-4} M) with (*R*)-limonene, an inversion of the CD sign of BOX_⊥ certainly took place but only very slowly at 20 °C to reach a plateau in 24 h (Figure 4c). Thus, the chiroptical memory^[5,9,21] of BOX_⊥ is long-lived, as expected from the large activation energy for racemization (vide ante). However, as beneficial for quick chiroptical sensing, a trace amount of THF, a weakly coordinating base, considerably shortened the time for thermodynamic equilibrium to be reached, without affecting the CD intensity finally attained.

By reference to the CD intensity at 458 nm of BOX_⊥, separated as the first fraction in chiral HPLC (Figure 2d), the enantiomeric excess of BOX_⊥ in limonene was estimated to be at most 3%. Therefore, the successful chiroptical sensing of limonene takes great advantage of the inherently large molecular ellipticity of enantiomerically pure BOX_⊥. A CPK model study predicted that BOX_⊥ is likely to adopt a rectangular shape, whose inner space (1 × 1 × 2 nm) can accommodate four to six molecules of limonene. The extraordinary large molecular ellipticity of BOX_⊥ implies that it might be distorted in an orthorhombic manner for minimization of the vacancy in the solvent-included inner space.

In conclusion, we have demonstrated that the zinc complex of a bisporphyrin bearing pyridyl groups, **1**, can chiroptically sense an asymmetric hydrocarbon, such as limonene, by forming a homochiral box-shaped tetrameric assembly, BOX_⊥. Chiroptical sensing can be performed readily by addition of **1** to limonene; because the BOX_⊥ formed is enantiomerically enriched, the optical purity and the absolute configuration of limonene can be determined. While the extent of the enantiomeric enrichment is small, the extremely large molecular ellipticity of chiral BOX_⊥ enables sensitive chiroptical visualization.

Experimental Section

Most reagents and solvents were used as received from commercial sources without further purification. (*R*)-Limonene (97% ee) and (*S*)-limonene (96% ee) were purchased from Aldrich. For column chromatography, Wakogel C-300HG (particle size 40–60 mm, silica), C-400HG (particle size 20–40 mm, silica), aluminum oxide 90 standardized (Merck), and Bio-Beads S-X1 (BIO RAD) were used. Methods for characterization and analysis are described in the Supporting Information.

Synthesis of compound 1: To a CH₂Cl₂ solution (20 mL) of the zinc complex of 5-(4-pyridyl)-15-(3,5-didodecyloxyphenyl)-10-(trimethylsilylbutadiynyl)porphyrin (70 mg, 69 μ mol) was added a THF solution of Bu₄NF (1.0 M, 100 μ L), and the mixture was stirred for 1 h at room temperature. Then, the reaction mixture was extracted with CHCl₃/H₂O, and the combined organic extract was dried over anhydrous Na₂SO₄ and concentrated to dryness. The residue was recrystallized from CH₂Cl₂/MeCN to give a green solid (54 mg). To a CH₂Cl₂/pyridine (100:1) solution (130 mL) of this residue were successively added *N,N,N',N'*-tetramethylethylenediamine (520 mg, 57 μ mol) and CuCl (440 mg, 4.48 mmol), and the mixture was stirred

for 15 min at room temperature. Then, the reaction mixture was extracted with CHCl₃/H₂O, and the combined organic extracts were dried over anhydrous Na₂SO₄ and concentrated to dryness. A CHCl₃ solution of this residue was treated with 6 N aq. HCl to allow demetalation, washed with aq. NaHCO₃ and water, dried over anhydrous Na₂SO₄, and then concentrated to dryness. The residue was subjected to size exclusion chromatography (SEC) with toluene as an eluent; the first fraction was collected and stirred in CHCl₃ with an excess amount of Zn(OAc)₂ for 1 h. Then, the reaction mixture was extracted with CHCl₃/H₂O, and the combined organic extracts were dried over anhydrous Na₂SO₄ and concentrated to dryness. Recrystallization of the residue from CHCl₃/MeCN gave **1** as green solid in 85% yield (42 mg, 24 μ mol). Free-base form of **1**: MALDI-TOF MS: *m/z*: 1758, [*M*+H]⁺ calcd for C₁₁₈H₁₃₆N₁₀O₄: 1759; UV/Vis (CHCl₃): λ_{max} = 466, 493, 624, 675 nm; ¹H NMR (500 MHz, CDCl₃): δ = −2.61 (s, NH), 0.83 (t, *J* = 6.8 Hz, Me), 1.23–1.38 (br, alkyl), 1.52 (t, *J* = 7.5 Hz, alkyl), 1.89 (t, *J* = 7.5 Hz, alkyl), 4.15 (t, *J* = 6.5 Hz, alkyl), 6.93 (s, Ar), 7.36 (d, *J* = 2.2 Hz, Ar), 8.12 (d, *J* = 5.7 Hz, Py), 8.80 (d, *J* = 5.0 Hz, pyrrole- β), 8.86 (d, *J* = 5.0 Hz, pyrrole- β), 9.02 (d, *J* = 5.0 Hz, pyrrole- β), 9.06 (d, *J* = 5.7 Hz, Py), 9.09 (d, *J* = 5.0 Hz, pyrrole- β), 9.18 (d, *J* = 5.0 Hz, pyrrole- β), 9.20 (d, *J* = 5.0 Hz, pyrrole- β), 9.62 (d, *J* = 5.0 Hz, pyrrole- β), 9.64 (d, *J* = 5.0 Hz, pyrrole- β), and 10.08 ppm (s, meso). **1**: MALDI-TOF MS: *m/z*: 1885, [*M*+H]⁺ calcd for C₁₁₈H₁₃₂N₁₀O₄Zn: 1885; UV/Vis (CHCl₃): λ_{max} (ϵ M^{−1} cm^{−1}) = 458 (154000), 485 (47100), 638 (30000), 666 (29400) nm; ¹H NMR (500 MHz, CDCl₃, 20 °C, BOX_⊥/BOX_{||} = 1:1): δ = 0.73–1.88 (br, alkyl), 2.14 (d, *J* = 10.5 Hz, Py), 2.75 (d, *J* = 10.5 Hz, Py), 4.02–4.10 (m, alkyl), 6.17 (d, *J* = 10.5 Hz, Py), 6.38 (d, *J* = 10.5 Hz, Py), 6.84 (s, Ar), 7.30 (s, Ar), 7.38 (s, Ar), 7.47 (d, *J* = 5.0 Hz, pyrrole- β), 7.73 (d, *J* = 5.0 Hz, pyrrole- β), 8.93 (d, *J* = 5.0 Hz, pyrrole- β), 8.94 (d, *J* = 5.0 Hz, pyrrole- β), 9.07 (d, *J* = 5.0 Hz, pyrrole- β), 9.14 (d, *J* = 5.0 Hz, pyrrole- β), 9.17 (d, *J* = 5.0 Hz, pyrrole- β), 9.27 (d, *J* = 5.0 Hz, pyrrole- β), 9.28 (d, *J* = 5.0 Hz, pyrrole- β), 9.45 (d, *J* = 5.0 Hz, pyrrole- β , BOX_{||}), 9.47 (d, *J* = 5.0 Hz, pyrrole- β , BOX_⊥), 9.75 (d, *J* = 5.0 Hz, pyrrole- β), 9.76 (d, *J* = 5.0 Hz, pyrrole- β), 10.05 (s, meso, BOX_⊥) and 10.06 ppm (s, meso, BOX_{||}).

Received: October 23, 2006

Published online: February 9, 2007

Keywords: chiroptical sensing · hydrocarbons · molecular recognition · porphyrinoids · self-assembly

- [1] a) Y. Masada, *Analysis of Essential Oils by Gas Chromatography and Mass Spectrometry*, Wiley, New York, **1967**; b) J. Ehlers, W. A. König, S. Lutz, G. Wenz, H. tom Dieck, *Angew. Chem.* **1988**, *100*, 1614–1615; *Angew. Chem. Int. Ed. Engl.* **1988**, *27*, 1556–1558; c) V. Schurig, H. P. Nowotny, *Angew. Chem.* **1990**, *102*, 969–986; *Angew. Chem. Int. Ed. Engl.* **1990**, *29*, 939–957; d) “Bioactive Volatile Compounds from Plants”: R. Teranishi, R. G. Buttery, H. Sugisawa, *ASC Symp. Ser.* **1993**, 525.
- [2] a) K. Kobayashi, Y. Asakawa, Y. Kikuchi, Y. Aoyama, *J. Am. Chem. Soc.* **1993**, *115*, 2648–2654; b) R. B. Prince, S. A. Barnes, J. S. Moore, *J. Am. Chem. Soc.* **2000**, *122*, 2758–2762; c) R. Paolesse, D. Monti, L. La Monica, M. Venanzi, A. Froio, S. Nardis, C. Di Natale, E. Martinelli, A. D’Amico, *Chem. Eur. J.* **2002**, *8*, 2476–2483; d) T. Kawasaki, H. Tanaka, T. Tsutsumi, T. Kasahara, I. Sato, K. Soai, *J. Am. Chem. Soc.* **2006**, *128*, 6032–6033.
- [3] a) A. Tsuda, H. Hu, R. Watanabe, T. Aida, *J. Porphyrins Phthalocyanines* **2003**, *7*, 388–393; b) A. Tsuda, H. Hu, R. Tanaka, T. Aida, *Angew. Chem.* **2005**, *117*, 4962–4966; *Angew. Chem. Int. Ed.* **2005**, *44*, 4884–4888.
- [4] a) J.-M. Lehn, A. Rigault, J. Siegel, J. Harrowfield, B. Cheverier, D. Moras, *Proc. Natl. Acad. Sci. USA* **1987**, *84*, 2565–2569; b) M. Cantuel, G. Bernardinelli, G. Muller, J. P. Riehl, C. Piguet, *Inorg.*

- Chem.* **2004**, *43*, 1840–1849; c) K. Zeckert, J. Hamacek, J.-M. Senegas, N. Dalla-Favera, S. Floquet, G. Bernardinelli, C. Piguet, *Angew. Chem.* **2005**, *117*, 8168–8172; *Angew. Chem. Int. Ed.* **2005**, *44*, 7954–7958; d) J. Lacour, V. Hebbe-Viton, *Chem. Soc. Rev.* **2003**, *32*, 373–382.
- [5] a) Y. Furusho, T. Kimura, Y. Mizuno, T. Aida, *J. Am. Chem. Soc.* **1997**, *119*, 5267–5268; b) Y. Mizuno, T. Aida, K. Yamaguchi, *J. Am. Chem. Soc.* **2000**, *122*, 5278–5285.
- [6] a) X. Huang, B. H. Rickman, B. Borhan, N. Berova, K. Nakanishi, *J. Am. Chem. Soc.* **1998**, *120*, 6185–6186; b) V. V. Borovkov, J. M. Lintuluoto, M. Fujiki, Y. Inoue, *J. Am. Chem. Soc.* **2000**, *122*, 4403–4407.
- [7] D. K. Smith, A. Zingg, F. Diederich, *Helv. Chim. Acta* **1999**, *82*, 1225–1241.
- [8] M. Takeuchi, T. Imada, S. Shinkai, *Angew. Chem.* **1998**, *110*, 2242–2246; *Angew. Chem. Int. Ed.* **1998**, *37*, 2096–2099.
- [9] E. Yashima, K. Maeda, Y. Okamoto, *Nature* **1999**, *399*, 449–451.
- [10] W.-S. Li, D.-L. Jiang, Y. Suna, T. Aida, *J. Am. Chem. Soc.* **2005**, *127*, 7700–7702.
- [11] Y. Shoji, K. Tashiro, T. Aida, *J. Am. Chem. Soc.* **2006**, *128*, 10690–10691.
- [12] a) A. G. Ogston, *Nature* **1948**, *162*, 963; b) T. D. Booth, D. Wahnnon, I. W. Wainer, *Chirality* **1997**, *9*, 96–98.
- [13] N. Harada, K. Nakanishi, *Acc. Chem. Res.* **1972**, *5*, 257–263.
- [14] a) D. P. Arnold, L. J. Nitschinsk, *Tetrahedron* **1992**, *48*, 8781–8792; b) D. P. Arnold, D. A. James, *J. Org. Chem.* **1997**, *62*, 3460–3469.
- [15] H. L. Anderson, *Chem. Commun.* **1999**, 2323–2330.
- [16] For characterization of self-assembly of **1** by reference to that of **2**,^[3] see the Supporting Information.
- [17] a) A. Tsuda, T. Nakamura, S. Sakamoto, K. Yamaguchi, A. Osuka, *Angew. Chem.* **2002**, *114*, 2941–2945; *Angew. Chem. Int. Ed.* **2002**, *41*, 2817–2821; b) I.-W. Hwang, T. Kamada, T. K. Ahn, D. M. Ko, T. Nakamura, A. Tsuda, A. Osuka, D. Kim, *J. Am. Chem. Soc.* **2004**, *126*, 16187–16198.
- [18] See the Supporting Information.
- [19] a) K. Yuki, Y. Okamoto, I. Okamoto, *J. Am. Chem. Soc.* **1980**, *102*, 6356–6358; b) C. Yamamoto, Y. Okamoto, *Bull. Chem. Soc. Jpn.* **2004**, *77*, 227–257.
- [20] The value of $|\Delta\epsilon|$ must be underestimated, since the molar absorption coefficient of BOX_⊥ at 458 nm, utilized for the calculation, reflects a certain contamination from achiral BOX_{||}.
- [21] a) L. J. Prins, F. D. Jong, P. Timmerman, D. N. Reinhoudt, *Nature* **2000**, *408*, 181–184; b) M. Ziegler, A. V. Davis, D. W. Johnson, K. N. Raymond, *Angew. Chem.* **2003**, *115*, 689–692; *Angew. Chem. Int. Ed.* **2003**, *42*, 665–668.